

Magnetic structures and properties of states in strongly frustrated Heisenberg antiferromagnets

R. S. Gekht

Institute of Physics, Siberian Branch of the Academy of Sciences

(Submitted 7 November 1992)

Zh. Eksp. Teor. Fiz. **102**, 1968–1982 (December 1992)

The magnetic structures and the properties of states in frustrated Heisenberg antiferromagnets are investigated. It is shown that frustrations induced in the system by additional spins result in a greater variety of phases with commensurate and incommensurate periods as well as in the appearance of aperiodic phases. The energy spectrum of the states is studied. It is established that the modulated $(0, Q)$ phase is unstable in a wide range of values of the parameters of the frustrations. The phase diagram of the states is constructed and the region where separate structures are locally degenerate is indicated.

1. INTRODUCTION

It is now well known that the effects of frustrations due to either competition of exchange interactions¹ or the lattice geometry (see, for example, Ref. 2 and the references cited there) play a very important role in different magnetic systems. Experimental and theoretical investigations have shown that in many respects their properties are fundamentally different from the corresponding unfrustrated systems. This difference is reflected primarily in the rich diversity of phases and phase transitions; it is due to the strong degeneracy and high sensitivity of the systems to different types of perturbing interactions.

Quantum effects in frustrated systems can alter the ground state decisively, essentially because the effective spin length can vanish completely.³ For this reason, in low-dimensional systems, where these effects are most pronounced, disordered states with zero site magnetization are possible in addition to the usual ordered states (Néel structures, spiral phases, etc.^{4,6}). Experimental evidence for the existence of such states is presented in numerous studies.^{7–11} Chandra and Doucot were the first to study this question theoretically.¹² It has been established that in square frustrated lattices (in contrast to the analogous problem for triangular lattices¹³) quantum fluctuations can destroy long-range order at zero temperatures even for systems with classical spins.

A great deal of attention has also been devoted in various studies to the character of the magnetic structure in compounds in which additional $3d$ -elements are either embedded in the crystal lattice or replace some cations of the main elements.^{14–16} In the present paper the structures and properties of the states of such systems are investigated. It is shown below that mixed phases of such materials induce an additional frustration channel. The result is that separate structures are strongly degenerate and unstable with respect to zero vibrations in a wide range of values of the parameters of two-dimensional magnetic systems. The problem considered here is described by the following Hamiltonian:

$$\mathcal{H} = J \sum_{r,a} S_r S_{r+a} + J' \sum_{r,d} S_r S_{r+d} + J_0 \sum_{r,d/2} S_r S_{r+d/2}, \quad (1)$$

where $J (> 0)$ is the antiferromagnetic interaction between the main magnetic ions along the edge of a square and J' and J_0 are interactions of either sign along the diagonal of the square. The first constant corresponds to interaction of the main spins and the second one corresponds to the interaction between the main and additional ions, located at the center of the square (nearest-spin interaction).

For $J_0 = 0$ the additional spins are free, and the main spins form a simple square lattice in which frustrations are induced by the antiferromagnetic interaction J' . For $j < 0.5$, where we have written $j = J'/J$, the ground state for large S is the standard Néel ordered state with two antiparallel sublattices. Conversely, for $j > 0.5$ each of the preceding sublattices decomposes into two antiparallel sublattices, forming a Néel state with four magnetic sublattices. For $j = 0.5$ the ground state is strongly degenerate: Quantum fluctuations destroy long-range order, and as a result the Néel structures can be separated from one another by an intermediate disordered phase.¹²

For $J_0 \neq 0$ additional frustrations arise in the system, irrespective of the sign of the exchange constant. For this reason it should be expected that such a system will have a richer phase diagram. The possible magnetic structures in the ground state are examined in Sec. 2. The spectrum of excitations of the structures found is investigated in Sec. 3. In the last section the phase diagram in the $S^{-1} - j_0$ plane is constructed for the special case $j > 0.5$.

2. MAGNETIC STRUCTURES IN THE GROUND STATE

In the ground state the energy of the spatially nonuniform structures with high spin S is

$$E = NS^2 J(\mathbf{Q})/2, \quad (2a)$$

where

$$J(\mathbf{k}) = J(\cos k_x + \cos k_y) + 2J' \cos k_x \cos k_y + 4J_0 \cos \frac{k_x}{2} \cos \frac{k_y}{2} \quad (2b)$$

and the lattice constant satisfies $a = 1$. Analysis shows that in the general case a frustrated Heisenberg system has five different phases, whose wave vectors \mathbf{Q} satisfy the condition

$\nabla_Q J(\mathbf{Q}) = 0$. The energy and the region of existence of these phases are given as follows ($j_0 = J_0/J$):

a) ferromagnetic phase ($Q = 0$):

$$E_1 = 2J(1+j+2j_0)S^2N, \quad (3a)$$

$$j_0 \leq -1, \quad j \leq 0;$$

$$j_0 \geq -2j-1, \quad j \geq 0,$$

b) antiferromagnetic phase ($Q_x = 0, Q_y = 2\pi$):

$$E_2 = 2J(1+j-2j_0)S^2N, \quad (3b)$$

$$j_0 \geq 1, \quad j \leq 0; \quad j_0 \geq 2j+1, \quad j \geq 0,$$

c) antiferromagnetic phase ($Q_x = Q_y = \pi$):

$$E_3 = -2J(1-j)S^2N, \quad (3c)$$

$$-1 \leq j_0 \leq 1, \quad j \leq 0;$$

$$2j-1 \leq j_0 \leq (1-4j^2)^{1/2}, \quad 0 \leq j \leq 0,5,$$

d) incommensurate phase IC_1 [$Q_x = 0, \cos Q_y / 2 = -j_0 / (1 + 2j)$],

$$E_4 = -2J \left(j + \frac{j_0^2}{1+2j} \right) S^2N, \quad (3d)$$

$$(1-4j^2)^{1/2} \leq j_0 \leq 2j+1, \quad 0 \leq j \leq 0,5;$$

$$-2j-1 \leq j_0 \leq 2j+1, \quad j \geq 0,5,$$

e) $2Q$ -incommensurate phase IC_2 [$Q_x = Q_y = Q, \cos Q = -(1+j_0)/2j$].

$$E_5 = -\frac{J}{2j} [(1+j_0)^2 - 4jj_0] S^2N, \quad (3e)$$

$$-2j-1 \leq j_0 \leq 2j-1, \quad 0 \leq j \leq 0,5.$$

The phase diagram of different states is displayed in Fig. 1. We note that the antiferromagnetic (π, π) phase is not unique in its region of existence. Since the field acting on an additional spin at the center of a square is zero, the system is locally degenerate and has a set of aperiodic states. Similarly, the incommensurate phase IC_1 also is not unique in its region of existence. As an example, Fig. 2 shows two states with the same energy: the standard spiral state and the noncollinear ferromagnetic state. In addition, it turns out that

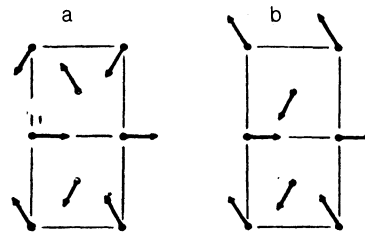


FIG. 2. State with the same energy in the classical case ($j_0 = 1, j = 0.5$): a—120-degree structure; b—noncollinear ferromagnetic structure.

aperiodic structures with the same energy are also possible in the region where this phase exists. The basic features of the system which are associated with this degeneracy will be examined below.

3. SPECTRUM OF EXCITATIONS OF STRUCTURES

We now investigate the energy spectrum of the states found. Let the magnetic structures of the ground state lie in the xz plane. We choose the axis of quantization of the local coordinate system along the direction of the spin in the corresponding structure, characterized by the wave vector \mathbf{Q} . Then the pair interaction $\mathbf{S}_i \cdot \mathbf{S}_j$ is represented in a spiral coordinate system (the primed spins) as follows:

$$\mathbf{S}_i \cdot \mathbf{S}_j = \cos \theta_{ij} S_i'^z S_j'^z + \frac{\cos \theta_{ij} - 1}{4} (S_i'^+ + S_j'^+ + S_i'^- S_j'^-) + \frac{\cos \theta_{ij} + 1}{4} (S_i'^- S_j'^+ + S_i'^+ S_j'^-) + \frac{\sin \theta_{ij}}{2} [(S_i'^+ + S_i'^-) S_j'^z - S_i'^z (S_j'^+ + S_j'^-)], \quad (4)$$

where $\theta_{ij} = Q(\mathbf{R}_i - \mathbf{R}_j)$ is the angle of rotation of the axis of the spiral between the sites i and j .

In the quadratic approximation in the Bose operators

$$S_i'^z = S - a_i^+ a_i, \quad S_i'^+ = (2S)^{1/2} a_i, \quad S_i'^- = (2S)^{1/2} a_i^+$$

the starting Hamiltonian has the form

$$\mathcal{H} = S^2 N_d \sum_{\alpha\beta} J_{\alpha\beta}(\mathbf{Q}) - 2S \sum_{\alpha\beta; k} J_{\alpha\beta}(\mathbf{Q}) a_{k\alpha}^+ a_{k\beta} + \frac{S}{2} \sum_{\alpha\beta; k} [J_{\alpha\beta}^+(\mathbf{k}) (a_{k\alpha}^+ a_{k\beta} + a_{k\alpha} a_{k\beta}^+) + J_{\alpha\beta}^-(\mathbf{k}) (a_{k\alpha}^+ a_{-k\beta}^+ + a_{k\alpha} a_{-k\beta})],$$

$$J_{\alpha\beta}^{\pm}(\mathbf{k}) = \frac{1}{2} [J_{\alpha\beta}(\mathbf{k} + \mathbf{Q}) + J_{\alpha\beta}(\mathbf{k} - \mathbf{Q})] \pm J_{\alpha\beta}(\mathbf{k}), \quad (5)$$

where N_d is the number of particles with spin S in the magnetic subsystem; the indices α and β characterize the number of magnetic subsystems; and

$$a_{k\alpha} = N_d^{-1/2} \sum_m a_{m\alpha} \exp(-ik\mathbf{R}_{m\alpha}).$$

In the expression (5) it is assumed that different ions have the same spin.

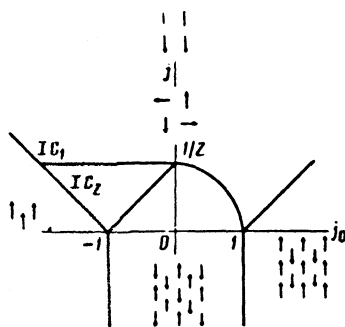


FIG. 1. Phase diagram of the ground state in the limit of large S : IC_1 —incommensurate $(0, Q)$ phase, IC_2 —incommensurate (Q, Q) phase.

3.1. Phases with commensurate period

It is well known that in a uniform ferromagnetic phase there are not zero-point vibrations and the quantum ground state is identical to the classical state. The simplest nonuniform collinear structure to investigate is the spectrum of excitations of the $(0, 2\pi)$ phase. In this phase the magnetic sublattices of the main spins ($\alpha, \beta = 1$) and the secondary spins ($\alpha, \beta = 2$) have an antiparallel orientation, so that the Fourier components of the exchange interactions have the form

$$\begin{aligned} J_{11}(\mathbf{k} \pm \mathbf{Q}) &= J_{11}(\mathbf{k}), \\ J_{12}(\mathbf{k} \pm \mathbf{Q}) &= -J_{12}(\mathbf{k}), \end{aligned} \quad (6a)$$

where

$$\begin{aligned} J_{11}(\mathbf{k}) &= 2J(\cos k_x + \cos k_y + 2j \cos k_x \cos k_y), \\ J_{12}(\mathbf{k}) &= 4J_0 \cos \frac{k_x}{2} \cos \frac{k_y}{2}. \end{aligned} \quad (6b)$$

Substituting these expressions into Eq. (5) and taking into account the fact that there is no interaction between the additional spins, $J_{22}(k) \equiv 0$, we obtain

$$\mathcal{H} = E_{cl} - 4J_0SN + 8J_0S \sum_k \alpha_k^+ M_k \alpha_k, \quad (7)$$

where E_{cl} is the same as E_2 from Eq. (3b), $\alpha_k^+ = (a_{k1}^+, a_{-k2})$ and

$$M_k = \begin{pmatrix} A_k & B_k \\ B_k & 1 \end{pmatrix}.$$

Here

$$\begin{aligned} A_k &= [J_0 - J - J' + J_{11}(\mathbf{k})/4]/J_0, \\ B_k &= -J_{12}(\mathbf{k})/(4J_0). \end{aligned}$$

After diagonalizing the quadratic Hamiltonian (7) we obtain

$$\begin{aligned} \mathcal{H} &= E_0 + 8J_0S \sum_{k,\alpha} \varepsilon_{k\alpha} c_{k\alpha}^+ c_{k\alpha}, \\ E_0 &= E_{cl} - 4J_0SN + 8J_0S \sum_k \varepsilon_{k1}, \end{aligned} \quad (8)$$

where $c_{k\alpha}^+$ is a new set of Bose operators and

$$\begin{aligned} \varepsilon_{k1} &= (1 - A_k + R_k)/2, \quad \varepsilon_{k2} = (A_k - 1 + R_k)/2; \\ R_k &= [(A_k + 1)^2 - 4B_k^2]^{1/2}. \end{aligned} \quad (9)$$

The spectrum of excitations ε_{k1} is linear near the points $\mathbf{k} = (0, 0)$ and $\mathbf{k} = (2\pi, 2\pi)$:

$$\varepsilon_{k1} = \frac{1}{2} \left(1 - \frac{1+2j}{j_0} \right)^{1/2} k.$$

As the interface between the initial phase and the modulated phase IC₁ is approached, additional softening of the spectrum occurs: the spin wave velocity

$$c \sim (j_0 - 2j - 1)^{1/2}$$

decreases and vanishes on the critical line $j_0 = 2j - 1$, on which, as a result, the spectrum near small k becomes quadratic.

The quantum reduction of the spin $\Delta S_\alpha = \langle a_\alpha^+ a_\alpha \rangle$ for the main and additional ions in the given $(0, 2\pi)$ phase is the same and is given in the form

$$\Delta S = \frac{1}{8\pi^2} \int \left(\frac{A_k + 1}{R_k} - 1 \right) d^2k. \quad (10)$$

As $j_0 - 2j + 1$ ($j \geq 0$) the quantum fluctuations grow and diverge logarithmically in the asymptotic limit:

$$\Delta S \sim \ln(j_0 - 2j - 1). \quad (11)$$

We now consider the antiferromagnetic (π, π) phase. In this case

$$\begin{aligned} J_{11}(\mathbf{k} \pm \mathbf{Q}) &= -2J(\cos k_x + \cos k_y) + 4J' \cos k_x \cos k_y, \\ J_{12}(\mathbf{k} \pm \mathbf{Q}) &= 4J_0 \sin \frac{k_x}{2} \sin \frac{k_y}{2}. \end{aligned} \quad (12)$$

Substituting the expressions (12) into Eq. (5) we obtain

$$\mathcal{H} = E_{cl} - 2JS(1-j)N + 4JS \sum_k \alpha_k^+ M_k \alpha_k, \quad (13)$$

where now E_{cl} is also E_3 in Eq. (3c); $\alpha_k^+ = (a_{k1}^+, a_{k2}, a_{-k1}, a_{-k2})$,

$$\begin{aligned} \alpha_k^+ &= (a_{k1}^+, a_{k2}^+, a_{-k1}, a_{-k2}), \\ M_k &= \begin{pmatrix} F_k & G_k \\ G_k & F_k \end{pmatrix}, \quad F_k = \begin{pmatrix} A_k & C_k^- \\ C_k^- & 0 \end{pmatrix}, \quad G_k = \begin{pmatrix} B_k & C_k^+ \\ C_k^+ & 0 \end{pmatrix}. \end{aligned} \quad (14)$$

Here

$$\begin{aligned} A_k &= 1 - j + j \cos k_x \cos k_y, \\ B_k &= -1/2 (\cos k_x + \cos k_y), \\ C_k^\pm &= -\frac{j_0}{2} \cos \frac{k_x \pm k_y}{2}. \end{aligned}$$

Diagonalizing the Hamiltonian (13) we obtain

$$\begin{aligned} \mathcal{H} &= E_0 + 8JS \sum_{k,\alpha} \varepsilon_{k\alpha} c_{k\alpha}^+ c_{k\alpha}, \\ E_0 &= E_{cl} - 2JS(1-j)N + 4JS \sum_k \varepsilon_{k\alpha}. \end{aligned} \quad (15)$$

The energy spectrum ε_k in Eq. (15) is given in the form

$$\begin{aligned} \varepsilon_{k\alpha} \equiv \varepsilon_k^\pm &= [1/2(A_k^2 - B_k^2) + (C_k^-)^2 - (C_k^+)^2 \pm R_k]^{1/2}, \\ R_k &= \{1/4(A_k^2 - B_k^2)^2 + (A_k^2 - B_k^2)[(C_k^-)^2 - (C_k^+)^2]\}^{1/2}. \end{aligned} \quad (16)$$

The spin-wave spectrum for the (π, π) structure is presented in Figs. 3b and c. The curves $\varepsilon_{k\alpha}$ are presented as a function of k_x for three values of k_y : $\pi/4$, $\pi/16$, and 0. The lower branch ε_{k1} characterizes the oscillation spectrum of the additional spins. For $j_0 = 0$ this branch vanishes, as it should. For $j_0 \neq 0$, however, the entire branch can vanish, if k_y or k_x is zero (curve 3, Fig. 3b). It is obvious that this fact reflects the local degeneracy of the classical ground state with respect to continuous rotations of the additional spins. The upper branch ε_{k2} , however, characterizes the oscillation

spectrum of the main spins and vanishes only at symmetric points of the Brillouin zone $\mathbf{k} = 0, \mathbf{k} = (\pi, \pi)$. Nevertheless, due to frustrations additional softening of the spectrum at the points $\mathbf{k} = (\pi, 0)$ (dashed line in Fig. 3c) and $\mathbf{k} = (0, \pi)$ is possible as j increases. If, however, $j_0 \neq 0$ holds due to a first-order phase transition into the neighboring phase the spectrum ε_{k_2} does not vanish.

In accordance with this behavior of the dispersion curves, the spin deviations of the main and additional ions at the lattice sites are significantly different. Calculations show that, as expected, the magnetic subsystem of the additional spins is completely disordered as a result of local degeneracy. At the same time, the magnetic subsystem consisting of the main spins is ordered everywhere except at the point $(j_0, j) = (0, 1/2)$ in the phase diagram in Fig. 1, where, like the Néel (π, π) state,¹² quantum fluctuations have a logarithmic divergence.

The quantum corrections to spin waves in the series expansion of \mathcal{H} up to $O(1/S^3)$ make ε_{k_1} nonzero for all orientations of the wave vector \mathbf{k} , including along the x and y axes. For this reason, the average spin for the additional ions will now also be different from zero, but its relative spin is small compared to S .

3.2. Phases with incommensurate period

The energy spectrum of incommensurate structures is more complicated and requires that the magnetic subsystem with the additional spins be divided into two systems (Fig. 4a), and as a result the indices α and β in the Hamiltonian (5) will run through the values 1, 2, and 3. We first investi-

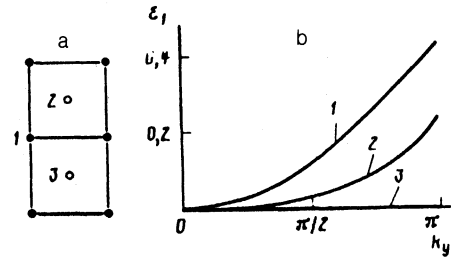


FIG. 4. a—Lattice with three types of sites: 1, 2, 3; b—lower branch of the excitation spectrum of the $(0, Q)$ phase for $j_0 = 1, j = 0.7$. $k_x = \pi/2$ (1), $\pi/6$ (2), and 0 (3).

gate the spectrum of the incommensurate phase IC_1 with wave vector $\mathbf{Q} = (0, Q)$, where $Q = 2 \cos^{-1}[-j_0/(1+2j)]$. Substituting into Eq. (5) the expression for $J_{11}(k)$ from Eq. (6b) and

$$J_{12}(\mathbf{k}) = 2J_0 \cos \frac{k_x}{2} \cos \frac{k_y}{2}, \quad J_{13}(\mathbf{k}) = J_{12}(\mathbf{k}), \quad (17)$$

$$(J_{22}(\mathbf{k}) = J_{23}(\mathbf{k}) = J_{33}(\mathbf{k}) = 0),$$

as well as the expressions for $J_{\alpha\beta}(k \pm Q)$ obtained from here, we have

$$\mathcal{H} = E' + JS \sum_{\mathbf{k}} \alpha_{\mathbf{k}}^+ M_{\mathbf{k}} \alpha_{\mathbf{k}}, \quad (18)$$

$$E' = -2J \left(j + \frac{j_0^2}{1+2j} \right) S(S+1)N.$$

Here $\alpha_{\mathbf{k}}^+ = (a_{k_1}^+, a_{k_2}^+, a_{k_3}^+, a_{-k_1}^+, a_{-k_2}^+, a_{-k_3}^+)$, and the matrix $M_{\mathbf{k}}$ has the same form as in Eq. (14), but its elements $F_{\mathbf{k}}$ and $G_{\mathbf{k}}$ are expressed as follows:

$$F_{\mathbf{k}} = \begin{pmatrix} A_{\mathbf{k}} & B_{\mathbf{k}}^- & B_{\mathbf{k}}^- \\ B_{\mathbf{k}}^- & D & 0 \\ B_{\mathbf{k}}^- & 0 & D \end{pmatrix}, \quad G_{\mathbf{k}} = \begin{pmatrix} C_{\mathbf{k}} & B_{\mathbf{k}}^+ & B_{\mathbf{k}}^+ \\ B_{\mathbf{k}}^+ & 0 & 0 \\ B_{\mathbf{k}}^+ & 0 & 0 \end{pmatrix}, \quad (19)$$

where

$$A_{\mathbf{k}} = 2[2j + \cos k_x + \delta^2(1+2j \cos k_x) \cos k_y], \quad (20)$$

$$B_{\mathbf{k}}^{\pm} = -j_0(\delta \pm 1) \cos \frac{k_x}{2} \cos \frac{k_y}{2},$$

$$C_{\mathbf{k}} = 2(\delta^2 - 1)(1+2j \cos k_x) \cos k_y,$$

$$D = 2j_0\delta, \quad \delta = j_0/(1+2j).$$

The Hamiltonian (18) is diagonalized by Bogolyubov's paraunitary transformation:¹⁷

$$IM(\mathbf{k})\mathbf{T}_n = \lambda_n \mathbf{T}_n. \quad (21)$$

Here $I = \text{diag}(1, 1, 1, -1, -1, -1)$ is a "para" unit matrix and $\mathbf{T}_n = (T_{1n}, T_{2n}, T_{3n}, T_{4n}, T_{5n}, T_{6n})$ are eigenvectors corresponding to the column matrices of the transformation T_{mn} from the operators $a_{\mathbf{k}}^+$ to the new operators $c_{\mathbf{k}}^+$.

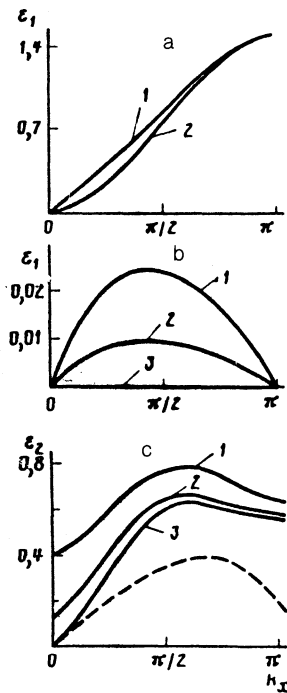


FIG. 3. Spectrum of spin-wave excitations: a— $\varepsilon_1(\mathbf{k})$ for the $(0, 2\pi)$ phase with $j_0 = 1.5, k_y = 0$. The curve 1 corresponds to $j = 0.15$ and curve 2 corresponds to $j = 0.24$; b, c— $\varepsilon_1(\mathbf{k})$ and $\varepsilon_2(\mathbf{k})$ for the (π, π) phase with $j_0 = 0.5$ and $j = 0.2$ (solid lines); the curves 1 correspond to $k_y = \pi/4$, the curves 2 correspond to $\pi/16$, and the curves 3 correspond to 0; the dashed line corresponds to $j_0 = 0.5, j = 0.4$, and $k_y = 0$.

It is easy to see that Eq. (21) has the solutions $\lambda_3 = D$ and $\lambda_6 = -D$, corresponding to the eigenvectors $\mathbf{T}_3 = 2^{-1/2} (0, 1, -1, 0, 0, 0)$ and $\mathbf{T}_6 = 2^{-1/2} (0, 0, 0, 0, 1, -1)$. In accordance with the orthogonality condition the remaining four eigenvectors have the following form:

$$\mathbf{T}_n = (u_1, u_2, u_3, v_1, v_2, v_3). \quad (22)$$

Substituting Eq. (22) into Eq. (21), we obtain an equation determining the vectors \mathbf{T}_n :

$$\begin{pmatrix} P_k(\lambda) & Q_k \\ Q_k & P_k(-\lambda) \end{pmatrix} \begin{pmatrix} u \\ v \end{pmatrix} = 0, \quad (23)$$

where $\mathbf{u} = (u_1, u_2)$, $\mathbf{v} = (v_1, v_2)$, and the matrices P_k and Q_k are defined as follows:

$$P_k(\lambda) = \begin{pmatrix} A_k^- \lambda & 2B_k^- \\ B_k^- & D - \lambda \end{pmatrix}, \quad Q_k = \begin{pmatrix} C_k & 2B_k^+ \\ B_k^+ & 0 \end{pmatrix}. \quad (24)$$

Solving Eq. (23), we find two eigenvalues λ :

$$\lambda_1 = -\lambda_2 = \lambda_-, \quad \lambda_3 = -\lambda_4 = \lambda_+, \quad (25a)$$

$$\lambda_{\pm} = [^{1/2}(\xi_k \pm \eta_k^{1/2})]^{1/2}.$$

Here

$$\begin{aligned} \xi_k &= A_k^2 - C_k^2 + 4[(B_k^-)^2 - (B_k^+)^2] + D^2, \\ \eta_k &= (A_k^2 - C_k^2 - D^2)^2 + 8(A_k^2 - C_k^2 + D^2)[(B_k^-)^2 - (B_k^+)^2] \\ &\quad + 16D[A_k(B_k^+)^2 - 2B_k^- B_k^+ C_k + A_k(B_k^-)^2]. \end{aligned} \quad (25b)$$

As a result, after diagonalization the Hamiltonian (18) assumes the form

$$\mathcal{H} = E_0 + 2JS \sum_{k\alpha} \varepsilon_{k\alpha} c_{k\alpha}^+ c_{k\alpha}, \quad (26)$$

$$E_0 = E' + JS \sum_{k\alpha} \varepsilon_{k\alpha},$$

where $\varepsilon_{k\alpha} = (\lambda_1, \lambda_2, \lambda_3)$.

Analysis of the dispersion relation $\varepsilon_{k_1} = \lambda_1$ shows that for $k_x = 0$ the expression for ξ_k in Eq. (25b) is equal to $\eta_k^{1/2}$ and thus the energy of the spin waves is zero for all values of k_y . Figure 4b shows the lower branch of ε_k as a function of k_y for different values of k_x . One can see that as k_x decreases the gapless spectrum ε_{k_1} is further softened near $k_x = 0$. As k_x decreases further, the region of mode softening becomes larger and in the limit $k_x = 0$ it covers the entire range of k_y .

For $j_0 \neq 0$ (see below) this means that the quantum fluctuations for the main spins

$$\Delta S_i = \frac{1}{4\pi^2} \int \{ [u_i(\lambda_i(\mathbf{k}))]^2 + [u_i(\lambda_s(\mathbf{k}))]^2 \} d^2k \quad (27)$$

diverge and the standard order breaks down everywhere the incommensurate $(0, Q)$ phase exists. Physically this is due to the presence of strong degeneracy caused by frustrations, as a result of which both globally and locally degenerate classical states are possible. Figure 5a shows as an example a set of states with $j_0 = 1$ and $j = 0.5$. One can see that the initial 120-degree structure is locally degenerate along the y axis, i.e., along the axis for which the dispersion branch ε_{k_1} vanishes for all values of k_y . The spins in the layer between the dashed lines can be simultaneously turned continuously

around axes parallel to these lines without a change in the energy. For this reason classical states which are aperiodic along the y axis are possible together with periodic states.

In order to follow clearly how the quantum fluctuations diverge in this phase, we introduce into the initial Hamiltonian (1) the additional term

$$\mathcal{H}_z = -H \sum_i (S_{iz}^2 + S_{is}^2), \quad (28)$$

where the trial field \mathbf{H} is oriented along the local z' axis and acts only on the additional spins. The introduction of such a term means that the elements of the matrix M_k will contain additional terms, namely, in F_k the term $D + h$, where $h = 2H/JS$, will replace D . As a result, the local degeneracy is removed and the spectrum of oscillations as a function of k_y is different from zero at $k_x = 0$. The curves $\Delta S = S$ for different values of h are displayed in Fig. 5b. As h decreases, with the exception of $j_0 = 0$ the quantum fluctuations grow, the nonmagnetic region becomes larger, and in the limit $h \rightarrow 0$ an ordered state is possible only if $j_0 = 0$. (Nonlinear effects, of course, can transform the phase diagrams $S^{-1}-j_0$; this question will be studied in the next section for $j > 0.5$).

At this point it is appropriate to note that if $j_0 = 0$, the additional spins are free and disordered and the main spins form a simple square lattice with antiparallel structure $[\mathbf{Q} = (0, \pi)]$, in which, naturally, there is no local degeneracy along the y axis because this axis is collinear. We also note that the value of S^{-1} for $j_0 = 0$ (Fig. 5b) is identical to the analogous value given in Ref. 12.

In the $2Q$ -incommensurate phase IC_2 [$Q_x = Q_y = Q$, $\cos Q = -(1 + j_0)/2j$] the Hamiltonian \mathcal{H} in the quadratic approximation in a_k^+ is given in the form (26), where, however,

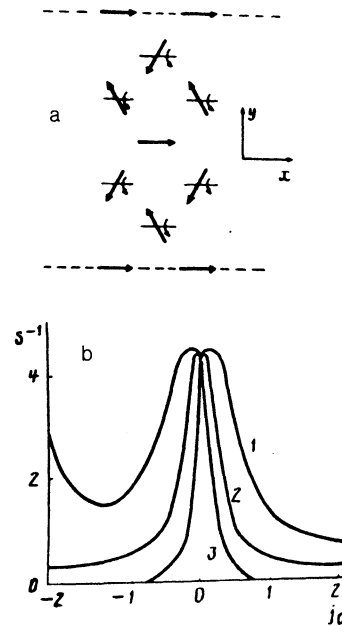


FIG. 5. a—Local degeneracy of the $(0, Q)$ phase along the y axis: $Q = 4\pi/3$; the arrows mark the direction of simultaneous rotation around the local axes; b—curves of S^{-1} versus j_0 for different values of the trial field h : 10^{-3} (1), 10^{-5} (2), and 10^{-7} (3). The curves are given for $j = 0.7$.

$$E' = -\frac{J}{2j} [(1+j_0)^2 - 4jj_0] S(S+1)N,$$

and the energy spectrum $\epsilon_{k\alpha} = (\lambda_1, \lambda_2, \lambda_3)$ in Eq. (25) is determined by the following expressions for A , B^\pm , C , and D :

$$\frac{A_k}{2} = 2\Delta - 2j_0 + (1-\Delta)(\cos k_x + \cos k_y) + 2j \cos(k_x - k_y) + 2j\Delta^2 \cos(k_x + k_y), \quad (29)$$

$$B_k^+ = -j_0(\Delta+1) \cos \frac{k_x + k_y}{2},$$

$$B_k^- = -j_0(\Delta-1) \cos \frac{k_x + k_y}{2} + 2j_0 \cos \frac{k_x - k_y}{2},$$

$$\frac{C_k}{2} = -(1+\Delta)(\cos k_x + \cos k_y) + 2j(\Delta^2 - 1) \cos(k_x + k_y),$$

$$D = 2j_0(\Delta-1); \quad \Delta = \frac{1+j_0}{2j}.$$

Analysis of the behavior of the spectrum $\epsilon_{k\alpha}$ shows that for $k_y = 0$ (for $k_x = 0$) the lower branch exhibits weak dispersion near the interface of the (Q, Q) and (π, π) phases. This occurs because the transition between these two phases is continuous and the system, just as in the (π, π) phase, is close to local degeneracy as before. Far from the interface, however, it becomes rigid, the energy of the wave excitations increases, and for this reason the quantum fluctuations cannot destroy long-range order in the (Q, Q) phase.

It is interesting to note that in the classical ground state the (Q, Q) phase is globally degenerate: Separate magnetic sublattices can be turned continuously relative to other sublattices. As an example Fig. 6a displays such a structure for

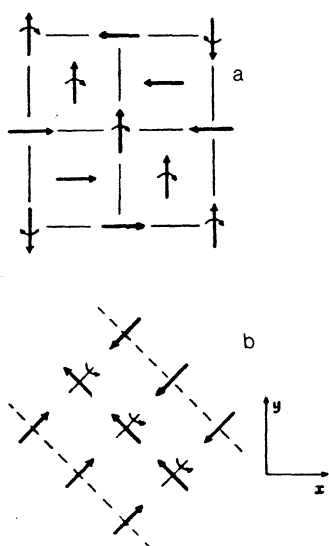


FIG. 6. a—Global continuous degeneracy in the phase (Q, Q) with $Q = \pi/2$; b—local degeneracy along the $(1, 1)$ direction for the point $(j_0 = -1, j = 0)$.

the case $Q = \pi/2$ ($j_0 = -1, 0 < j \leq 0.5$). Quantum fluctuations remove the continuous degeneracy, leaving only the state with either $Q = \pi/2$ or $Q = 3\pi/2$. At the corner point of the phase diagram in Fig. 1 ($j_0 = -1, j = 0$) states with any Q are possible. Such states are locally degenerate in the direction $(1, 1)$, as a result of which the quantum fluctuations diverge at this point.

4. PHASE DIAGRAM

We now construct the phase diagram S^{-1} versus j_0 in the most interesting region $j > 0.5$. In order to construct this diagram for all values of S we employ the method of Schwinger bosons (mean-field approximation).¹⁸ The spin operators in the Schwinger representation are replaced by two bosons

$$S_i = \frac{1}{2} b_{i\sigma}^+ \sigma_{\sigma\sigma'} b_{i\sigma'}, \quad b_{i\sigma}^+ b_{i\sigma} = 2S \quad (30)$$

where σ are the Pauli matrices, so that the pair interaction $S_i S_j$ is biquadratic in $b_{i\sigma}$. In transforming to a spiral coordinate system it is convenient to represent $S_i S_j$ in the vector form

$$S_i S_j = \frac{1}{2} (\cos \theta_{ij} + 1) S_i' S_j' + \frac{1}{2} (\cos \theta_{ij} - 1) \times [S_i' S_j' - 2(S_i' \mathbf{k})(S_j' \mathbf{k})] + \sin \theta_{ij} \mathbf{k} [S_i' S_j'], \quad (31)$$

where \mathbf{k} is a unit vector along the axis of the spiral (the y axis), instead of in the form (4). Then the initial Hamiltonian, written in terms of Schwinger bosons in a local coordinate system, is equivalent at the mean-field level to the Hamiltonian with BCS pairing:¹⁹

$$\mathcal{H}_{BCS} = \frac{1}{4} \sum_{\mathbf{k}, \mathbf{k}'} (\mathcal{T}_{\mathbf{k}\mathbf{k}'}^+ D_{\mathbf{k}}^+ D_{\mathbf{k}'} - \mathcal{T}_{\mathbf{k}\mathbf{k}'}^- B_{\mathbf{k}}^+ B_{\mathbf{k}'} - NJ(Q) S^2/2). \quad (32)$$

Here

$$\mathcal{T}_{\mathbf{k}\mathbf{k}'}^{\pm} = \frac{1}{2} \left\{ J(\mathbf{k} + \mathbf{k}') \pm \frac{1}{2} [J(\mathbf{k} + \mathbf{k}' + \mathbf{Q}) + J(\mathbf{k} + \mathbf{k}' - \mathbf{Q})] \right\}, \quad (32a)$$

where the index s denotes symmetrization with respect to \mathbf{k} and \mathbf{k}' , and the indices α and β for the different subsystems are dropped. The first and second terms in Eq. (32) are purely ferromagnetic and antiferromagnetic pairing potentials, respectively, and

$$B_{\mathbf{k}}^+ = b_{\mathbf{k}\sigma}^+ b_{-\mathbf{k}-\sigma}^+, \quad \text{and} \quad D_{\mathbf{k}}^+ = b_{\mathbf{k}\sigma}^+ b_{\mathbf{k}\sigma}$$

are the triplet Cooper and singlet particle-hole pairing fields for Schwinger bosons.

We now examine in greater detail S^{-1} as a function of j_0 at the transition from the disordered phase into the antiferromagnetic $(0, 2\pi)$ phase. In terms of Schwinger bosons the Hamiltonian (1) is

$$\mathcal{H} = \frac{1}{2} \sum_{i,j} J_{ij}^{11} [D_{i+1j}^+ D_{i1j} - S(S+1)] - \frac{1}{2} \sum_{i,j} J_{ij}^{12} (B_{i+2j}^+ B_{i+2j} - S^2), \quad (33)$$

Performing the mean-field decoupling in Eq. (33)

$$\langle D_{1i1j}^+ \rangle = 2\alpha_{1i1j}, \quad \langle B_{1i2j}^+ \rangle = 2\gamma_{1i2j}$$

and replacing the local coupling $b_{i\sigma}^+ b_{i\sigma} = 2S$ by the global coupling $\sum b_{i\sigma}^+ b_{i\sigma} = 2NS$, we obtain

$$\begin{aligned} \mathcal{H} = E_j + \sum_k (h_k - \lambda) (b_{k1\uparrow}^+ + b_{k1\downarrow}^+ + b_{-k1\downarrow} b_{-k1\uparrow}^+) \\ - \sum_k \lambda (b_{k2\uparrow}^+ + b_{k2\downarrow}^+ + b_{-k2\downarrow} b_{-k2\uparrow}^+) - \sum_k \Delta_k (b_{k1\uparrow}^+ + b_{-k2\downarrow}^+ + b_{k1\downarrow} b_{-k2\uparrow}^+). \end{aligned} \quad (34)$$

Here

$$\begin{aligned} E_c/N = 2\lambda(S + 1/2) - 2S(S+1)(J+J') \\ + 2J_0 S^2 - 4(J\alpha^2 + J'\beta^2 - J_0\gamma^2) \end{aligned}$$

and λ is a Lagrange multiplier. The quantities h_k and Δ_k are determined as follows:

$$\begin{aligned} h_k = 4J\alpha(\cos k_x + \cos k_y) + 8J'\beta \cos k_x \cos k_y, \\ \Delta_k = 8J_0\gamma \cos \frac{k_x}{2} \cos \frac{k_y}{2}, \end{aligned} \quad (35)$$

where α and β are equal to α_{1i1j} for the nearest and second-nearest (to the main) spins, respectively, and $\gamma = \gamma_{1i2j}$ for the nearest of the main and additional spins.

After the Hamiltonian (34) is diagonalized, the total ground-state energy has the form

$$\begin{aligned} E_0 = E_c - \lambda N/2 + \sum_k E_k, \\ E_k = 1/2(R_k - h_k), \quad R_k = [(h_k - 2\lambda)^2 - 4\Delta_k^2]^{1/2}. \end{aligned} \quad (36)$$

Minimizing E_0 with respect to α , β , γ , and λ , we obtain the following self-consistent equations for these quantities:

$$\begin{aligned} \alpha &= \frac{1}{16\pi^2} \int \frac{\tilde{h}_k}{R_k} (\cos k_x + \cos k_y) d^2k, \\ \beta &= \frac{1}{8\pi^2} \int \frac{\tilde{h}_k}{R_k} \cos k_x \cos k_y d^2k, \\ \gamma &= \frac{1}{2\pi^2} \int \frac{\Delta_k}{R_k} \cos \frac{k_x}{2} \cos \frac{k_y}{2} d^2k, \\ S + \frac{1}{4} &= \frac{1}{8\pi^2} \int \frac{\tilde{h}_k}{R_k} d^2k, \quad \tilde{h}_k = h_k - 2\lambda. \end{aligned} \quad (37)$$

In the disordered state, when S is small, the energy spectrum contains a gap (the spin waves are "massive"). In the presence of such a gap the system will not have long-range order for all S . However, if the gap vanishes for some S , Bose condensation occurs and long-range order is realized in the system. The latter will occur for fixed λ in the expression (36) for the energy spectrum E_k . Solving next the first three self-consistent equations in Eq. (37), we find α , β , and γ and substitute the obtained values into the last equation for S . The critical curve of S^{-1} versus j_0 for $j = 0.7$ is presented in Fig. 7a. In this figure the dashed line depicts the curve of S^{-1} versus j_0 obtained in the linear spin-wave approximation [the formula (10)]. Comparing these two curves shows that

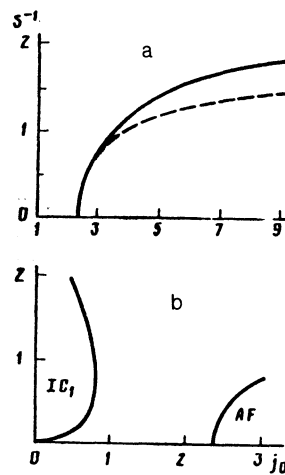


FIG. 7. Phase diagram in the $S^{-1}-j_0$ plane for $j = 0.7$: a—boundary of the $(0, 2\pi)$ phase; the solid line was obtained in the self-consistent approximation with Schwinger bosons and the dashed line was obtained in the spin-wave approximation; b—phase diagram constructed by the method of Schwinger bosons (self-consistent approximation); AF—antiferromagnetic $(0, 2\pi)$ phase.

for large S the solid and dashed lines are indistinguishable. The difference in their behavior becomes appreciable for $S < 1$: The curve constructed in the linear spin-wave approximation lies everywhere below the curve obtained in the self-consistent approximation with Schwinger bosons; i.e., nonlinear quantum effects enlarge the range of existence of the antiferromagnetic $(0, 2\pi)$ phase.

Similar calculations of S^{-1} versus j_0 were also performed by the Schwinger boson method for the case of the incommensurate $(0, Q)$ phase. The mean-field parameters were determined self-consistently from the following equations (the indices α and β for the subsystems are dropped):

$$\begin{aligned} h_k &= \frac{1}{8\pi^2} \int \mathcal{F}_{kk'} + \frac{h_{k'} - \lambda}{E_{k'}} d^2k', \\ \Delta_k &= \frac{1}{8\pi^2} \int \mathcal{F}_{kk'} - \frac{\Delta_{k'}}{E_{k'}} d^2k', \\ S + \frac{1}{2} &= \frac{1}{8\pi^2} \int \frac{h_k - \lambda}{E_k} d^2k, \end{aligned} \quad (38)$$

where $\mathcal{F}_{kk'}$ are given by Eq. (32a) and E_k is the energy spectrum determined by diagonalizing the mean-field Hamiltonian (for example, for the case $\alpha = \beta = 1$ it has the simple form $E_k = [(h_k - \lambda)^2 - \Delta_k^2]^{1/2}$).

Numerical analysis shows that in contrast to the linear spin-wave theory the phase diagram $S^{-1}-j_0$ contains a finite region of the $(0, Q)$ phase (Fig. 7b). The curve itself is reminiscent of the curve of S^{-1} versus j ($j_0 = 0$) constructed in Ref. 20 (see also Ref. 21) for the Néel $(0, \pi)$ phase. In the present case, however, the ordered phases are separated from one another by an intermediate disordered state for all S ; this is obviously largely due to the local symmetry of the classical state because of the additional frustration channel when $j_0 \neq 0$. It is also evident from the behavior of the curves in Fig. 7b that as S decreases, the nonlinear effects first enlarge the range in which the incommensurate phase exists

and only later, at some critical value of S^{-1} , when the spin is sufficiently small and quantum fluctuations are large, does this region shrink.

5. CONCLUSIONS

Thus possible states on two-dimensional lattices were investigated for a new frustrated system consisting of spins of two types. It was shown that the additional frustrations induced in such a system give rise to strong degeneracy of the ground state for large S . The energy spectrum of different phases was calculated. It was established that in the $(0, 2\pi)$ phase with commensurate period the lower branch of the spectrum ε_k undergoes additional softening as the boundary with the incommensurate $(0, Q)$ phase is approached. At the phase $(0, Q)$ itself the energy of the spin waves along definite directions of \mathbf{k} may turn into zero, regardless of the magnitude of the wave vector. This happens because of the existence of local degeneracy in the system. For this reason, the classical state $(0, Q)$ for $Q \neq \pi$ admits both periodic and aperiodic structures. In the linear approximation the quantum fluctuations for the $(0, Q)$ phase diverge in the entire region of its existence and such divergence is absent, as it should be, only in particular case of the collinear $(0, \pi)$ structure. Nonlinear effects significantly change the phase diagram: For values of Q close to π the incommensurate structure stabilizes at finite values of S . Nevertheless, in a wide region of the phase diagram $S^{-1} - j_0$ an ordered state is impossible for any S .

In the antiferromagnetic (π, π) phase the spin-wave energy also vanishes for arbitrary k if k_x or k_y is zero. This branch of the frequency spectrum corresponds to the additional (dopant) ions. The magnetic structure formed by them is locally degenerate for large S and, as a result of this, the zero-point vibrations diverge. However, quantum corrections to the spin-wave spectrum remove this divergence.

The $2Q$ -incommensurate phase does not have local degeneracy in the classical case, if $j > 0$ holds. Instead, global degeneracy, associated with continuous rotation of the mag-

netic sublattices relative to one another, is present. At the boundary of the phase, however, the classical ground state is locally degenerate at the corner point ($j_0 = -1, j = 0$).

In conclusion, I thank V. A. Ignatchenko, V. V. Val'kov, A. F. Sadreev, and N. V. Fedoseeva for helpful discussions and V. V. Grishin for assistance in the numerical calculations.

¹Yu. A. Izyumov, Usp. Fiz. Nauk **144**, 439 (1984) [Sov. Phys. Usp. **27**(11), 845 (1984)].

²R. S. Gekht and V. I. Ponomarev, Phase Transitions A **20**, 27 (1990); R. S. Gekht, Usp. Fiz. Nauk **159**, 261 (1989) [Sov. Phys. Usp. **32** (10), 871 (1989)].

³P. Fazekas and P. W. Anderson, Phil. Mag. **30**, 423 (1974).

⁴Yu. A. Izyumov and V. M. Laptev, Zh. Eksp. Teor. Fiz. **88**, 165 (1985) [Sov. Phys. JETP **61**, 95 (1985)].

⁵R. S. Gekht, Zh. Eksp. Teor. Fiz. **93**, 255 (1987) [Sov. Phys. JETP **66** (1), 147 (1987)].

⁶S. S. Aplesin and R. S. Gekht, Zh. Eksp. Teor. Fiz. **95**, 2163 (1989) [Sov. Phys. JETP **68** (6), 1250 (1989)].

⁷J. D. Reger and A. P. Young, Phys. Rev. B **37**, 549, 5978 (1988).

⁸D. A. Huse and V. Elser, Phys. Rev. Lett. **60**, 2531 (1988).

⁹S. Chakravarty, B. I. Halperin, and D. R. Nelson, Phys. Rev. Lett. **60**, 1057 (1988).

¹⁰M. Gross, E. Sanchez-Velasco, and E. Siggia, Phys. Rev. B **39**, 2484 (1989).

¹¹J. D. Reger, J. A. Riera, and A. P. Young, J. Phys. C **1**, 1955 (1989).

¹²P. Chandra and B. Doucot, Phys. Rev. B **38**, 9335 (1988).

¹³I. Ritchy, P. Chandra, and P. Coleman, Phys. Rev. Lett. **64**, 2583 (1990).

¹⁴J. M. Tarascon, P. Bardoux, P. F. Miceli *et al.*, Phys. Rev. B **37**, 7458 (1988).

¹⁵P. F. Miceli, J. M. Tarascon, L. H. Greene *et al.*, Phys. Rev. B **37**, 5932 (1988).

¹⁶T. Kajitani, K. Kusaba, M. Kikuchi, Y. Syono, and M. Hirabayashi, Tech. Report of ISSP, Roppongo, Minato-ku (1992), No. 2163.

¹⁷J. H. P. Colpa, Physica A **93**, 327 (1978).

¹⁸D. P. Arovos and A. Auerbach, Phys. Rev. B **38**, 316 (1988).

¹⁹P. Chandra, P. Coleman, and A. I. Larkin, J. Phys. Condens. Matter **2**, 7933 (1990).

²⁰F. Mila, D. Poilblanc, and C. Bruder, Phys. Rev. B **43** (1991).

²¹H. Nishimori and Y. Saika, J. Phys. Soc. Japan **59**, 4454 (1990).

Translated by M. E. Alferieff